HYDROLOGICAL PROCESSES
Hydrol. Process. **30**, 1676–1690 (2016)
Published online 14 December 2015 in Wiley Online Library
(wileyonlinelibrary.com) DOI: 10.1002/hyp.10726

A 477-year dendrohydrological assessment of drought severity for Tsable River, Vancouver Island, British Columbia, Canada

Bethany Coulthard* and Dan J. Smith

University of Victoria Tree-Ring Laboratory, Department of Geography, University of Victoria, Victoria, BC, Canada

Abstract:

Summer streamflow droughts are becoming more severe in many watersheds on Vancouver Island, British Columbia, as a result of climate warming. Small coastal basins that are the primary water source for most communities and essential to Pacific salmon populations have been particularly affected. Because the most extreme naturally occurring droughts are rarely captured within short instrumental records water managers likely underestimate, and are unprepared for, worst-case scenario low flows. To provide a long-term perspective on recent droughts on Vancouver Island, we developed a 477-year long dendrohydrological reconstruction of summer streamflow for Tsable River based on a network of annual tree-ring width data. A novel aspect of our study is the use of conifer trees that are energy limited by spring snowmelt timing. Explaining 63% of the instrumental streamflow variability, to our knowledge the reconstruction is the longest of its kind in British Columbia. We demonstrate that targeting the summer streamflow component derived from snowmelt is powerful for determining drought-season discharge in hybrid runoff regimes, and we suggest that this approach may be applied to small watersheds in temperate environments that are not usually conducive to dendrohydrology. Our findings suggest that since 1520, 21 droughts occurred that were more extreme than recent 'severe' events like those in 2003 and 2009. Recent droughts are therefore not anomalous relative to the ~400-year pre-instrumental record and should be anticipated within water management strategies. In coming decades, worst-case scenario natural droughts compounded by land use change and climate change could result in droughts more severe than any since 1520. The influence of the Pacific Decadal Oscillation on instrumental and modelled Tsable River summer streamflow is likely linked to the enhanced role of snowmelt in determining summer discharge during cool phases. Copyright © 2015 John Wiley & Sons, Ltd.

KEY WORDS dendrohydrology; drought; low flows; water management; Vancouver Island; British Columbia

Received 4 May 2015; Accepted 21 October 2015

INTRODUCTION

British Columbia's (B.C.) temperate rainforest coast is considered water-rich, but seasonal water scarcity and streamflow drought often occur during summer when demand for water is highest and storage is limited (Stephens *et al.,* 1992). In 2014 and 2015 many streams experienced droughts that were more severe than any on record (B.C. Ministry of Forests, Lands and Natural Resource Operations, 2014; B.C. River Forecast Centre, 2015). Climate warming has triggered earlier, lower, longer, and more frequent low-flows throughout the coastal region (Rodenhuis *et al.,* 2007), and the impact of worsening droughts on human water use, stream ecology, and the survival of Pacific salmon is recognized by the provincial government as a critical environmental management challenge (B.C. Ministry of Environment, 2013).

'Hybrid' runoff regimes are the primary water source for most towns, municipalities, and First Nations communities on Vancouver Island, B.C., and are also the most vulnerable to summer water shortages (Rodenhuis *et al.,* 2007). Both snowmelt and rainfall contribute substantially to annual streamflow in hybrid watersheds (Eaton and Moore, 2010). The likelihood of protracted drought under future climate conditions makes an accurate understanding of worst-case scenario droughts, based on long-term natural variability, crucial for effective water management in these basins (Pike *et al.,* 2010).

The purpose of our research was to develop a multi-century summer discharge (Q) record for a small hybrid watershed on southeastern Vancouver Island, and to interpret the severity of recent droughts within the context of that record. We used a dendrohydrological approach, where climate-sensitive tree-ring (TR) width records serve as proxies for climate in a paleo-hydrological model (Loaiciga *et al.,* 1993). Detection of recent environmental change often requires these long-term records because natural climatic patterns, such as the Pacific Decadal Oscillation (PDO), persist over multiple decades and can obscure climate change effects (Moore *et al.,* 2007).

*Correspondence to: Bethany Coulthard, University of Victoria Tree-Ring Laboratory, Department of Geography, University of Victoria, Victoria, British Columbia, Canada.
E-mail: bethanyc@uvic.ca

While streamflow reconstructions based on TR data have been developed for drought-sensitive regions world-wide, applying traditional dendrohydrological approaches to a small hybrid watershed in a temperate environment is problematic. First, very flashy rainfall-driven runoff is often a major contributor to total annual streamflow in coastal B.C. (Eaton and Moore, 2010). Dendrohydrological models usually target annual discharge in large watersheds where both runoff and annual radial tree growth are relatively unresponsive to 'flashy' rainfall events (Pederson *et al.,* 2001; Boninsegna *et al.,* 2009; Meko and Woodhouse, 2010; Yang *et al.,* 2010; Margolis *et al.*, 2011; Sauchyn *et al.,* 2014). Second, trees on Vancouver Island are rarely moisture stressed, although the radial growth of some species is sensitive to winter precipitation as a result of the energy-limiting role of deep snowpacks (Marcinkowski *et al*., In press). Dendrohydrological studies are usually conducted in arid environments using trees whose radial growth is limited by rainfall or snowmelt-derived soil moisture, which directly influences runoff (Woodhouse *et al.,* 2006). We circumvent these problems by targeting low-flow season streamflow in our reconstruction, a time of year when runoff is significantly less flashy, is primarily driven by snowmelt, and is most important for drought management (Smith and Laroque, 1998).

We hypothesized that summer discharge in a small hybrid basin on Vancouver Island is driven by regional snowmelt variations to the extent that TR records that are energy-limited by snow could serve as proxies for climate in a dendrohydrological reconstruction of streamflow. To date, paleohydrological efforts in B.C. have explored the utility of annual TR width and density records as proxies for winter and summer temperature and snow water equivalent (SWE) for reconstructing summer-season and mean water year runoff in nival and glacial watersheds (Gedalof *et al.*, 2004; Watson and Luckman, 2005; Hart *et al.*, 2010; Starheim *et al.*, 2013). No prior attempt has been made to develop seasonal reconstructions of the hybrid streams that are most susceptible to drought in coming decades.

We use the term 'drought' to mean streamflow drought, or below-normal stream discharge, a component of hydrological drought that often also coincides with reduced groundwater availability (Van Loon and Laaha, 2015). Consistent with B.C. government management practices, 'drought' refers to below-normal stream runoff persisting over a period of consecutive months (B.C. Ministry of Environment, 2013).

RESEARCH BACKGROUND

Large precipitation and temperature gradients characterize most watersheds on Vancouver Island. Winter storms originating in the North Pacific Ocean bring moisture to the west coast of the island, where orographic lift results in deep snowpacks at high elevation and large quantities of rain in lowland areas (Stahl *et al.*, 2006). Rain shadow effects on the east side of Vancouver Island result in drier conditions in lowland coastal regions (Rodenhuis *et al.,* 2007). Summers are warm and dry, and dominated by persistent high-pressure systems (Rodenhuis *et al.,* 2007). Seasonal hydroclimatic patterns are moderated by synoptic-scale inter-annual and decadal modes of climate variability stemming from ocean–atmosphere interactions in the Pacific Basin, of which the PDO, the El Niño Southern Oscillation (ENSO), and the Pacific North America (PNA) pattern have a particular influence on regional streamflow (Kiffney *et al.*, 2002).

Hybrid streams on Vancouver Island are found primarily in mid-elevation coastal and near-coastal areas where mean watershed elevations are not high enough to be fully nival (Eaton and Moore, 2010). Hybrid streams experience highest mean monthly flows during winter rains, followed by a significant pulse of runoff from snowmelt in spring. Lowest monthly flows occur during summer when discharge is governed by snow meltwater inputs, nominal summer precipitation inputs, and losses related to high summer air temperatures and evaporation (Eaton and Moore, 2010). Snowmelt can significantly recharge deep groundwater flow pathways to augment summer baseflow in the study region, even if only a small snow fed headwater is present (Moore *et al.,* 2007; Beaulieu *et al.,* 2012). Above average minimum summer discharge is therefore often coincident with deep snowpacks that develop during cool and wet La Niña years, especially when enhanced by cold phases of the PDO (Fleming *et al.,* 2007). The proportion of rainfall-derived *versus* snowmelt-derived runoff varies from year to year in accordance with fluctuations in winter temperature, so that annual flows in hybrid regimes can be 'more pluvial' or 'more nival' in any given year (Moore *et al.,* 2007). A high between-year range in monthly flow totals is typical (Moore *et al.,* 2007).

In the south coastal region of B.C., annual minimum streamflow has decreased in hybrid watersheds over the last 30 years, with low-flow magnitudes projected to decline by up to 50% by the end of the century as a result of seasonal climate trends (Rodenhuis *et al.,* 2007; Mantua *et al.,* 2010). Winters have become milder and wetter, with less winter precipitation falling as snow and more as rain, and more frequent rain-on-snow events. As a result, less snow meltwater is available to buffer low stream discharge during the dry summer months (Pike *et al.*, 2010). Projections suggest that nival flow contributions will weaken or become non-existent, eventually shifting many hybrid systems to more pluvial regimes (Eaton and Moore, 2010). Summers have become warmer and drier additionally drawing-down summer flows (Pike *et al.,* 2010).

STUDY SITE

The Tsable River watershed is a small (113 km^2) hybrid basin located on the eastern slopes of the Beaufort Range on central Vancouver Island, in the rainshadow of the Vancouver Island Ranges (Figure 1). With a maximum basin elevation of around 1500 m asl, a significant portion of precipitation within the watershed falls as snow above 1000 m asl (Eaton and Moore, 2010). Tsable Lake (~1 km^2) and several smaller lakes are located with the basin. Draining east to the Strait of Georgia, the lower reaches of the watershed are located within the dry Coastal Douglas Fir Zone, transitioning from the Coastal Western Hemlock Zone, to the Mountain Hemlock Zone and Alpine Tundra Zone with increasing elevation (Klinka *et al.*, 1991). At high elevation (1000–1500 m asl) the growing season is short and cool, with very deep snowpacks often persisting into the spring and summer. Mountain hemlock (TM; *Tsuga mertensiana* (Bong.) Carrière) trees are dominant, with subalpine fir (*Abies lasiocarpa* (Hook.) Nutt.) and amabilis fir (AA; *Abies amabilis* (Doug.) ex. Louden) trees occasionally co-dominant. Industrial logging is the main land use in the watershed.

Highest total monthly discharge in Tsable River occurs from November through January, with spring snowmelt causing a distinct pulse of runoff in May (Figure 2; Eaton and Moore 2010). Analysis of annual hydrographs provides a comparison between years dominated by winter rainfall- *versus* summer snowmelt-derived runoff (Figure 2). Lowest flows occur in July through September (Figure 2). In recent years, Tsable River summer baseflow has been far below optimum for the river's populations of chum, coho, and pink salmon, and resident and anadromous steelhead and cutthroat trout (B.C. Conservation Foundation 2006). Despite conservation efforts, low-flows have degraded stream habitat to the extent that the wild steelhead stock has likely been extirpated since the early 2000s (Lill, 2002; Silvestri, 2004).

DATA AND METHODS

Hydrometric and climate data

Only three hybrid streams on Vancouver Island have >50 years of natural and continuous instrumental data. Tsable River was selected for this study because it is the hybrid stream with the longest continuous natural hydrometric record (1960–2009), and the watershed does not contain large natural water storage features such as lakes and wetlands. We downloaded monthly discharge data for Tsable River from the Water Survey of Canada (http://www.wsc.ec.gc.ca/applications/H2O/index-eng.cfm). Missing values (1% of the data) were replaced with long-term monthly means (station code 08HB024; gauge location latitude: 49.517, longitude: −124.841, elevation: 1 m asl). We used the average flow from July to August for our reconstruction because the regional hydrological literature suggests that stream discharge is significantly correlated with previous winter SWE during that season (Rodenhuis *et al.,* 2007; Eaton and Moore, 2010). The July–August streamflow data, hereinafter 'summer

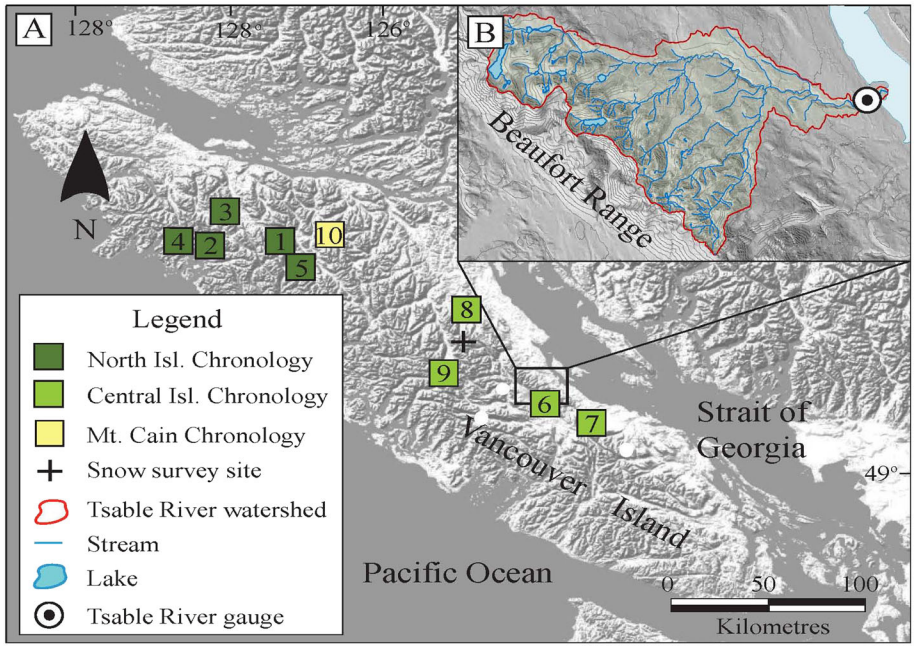

Figure 1. Map of the study area. (A) Vancouver Island. (B) Tsable River watershed 263 × 186 mm

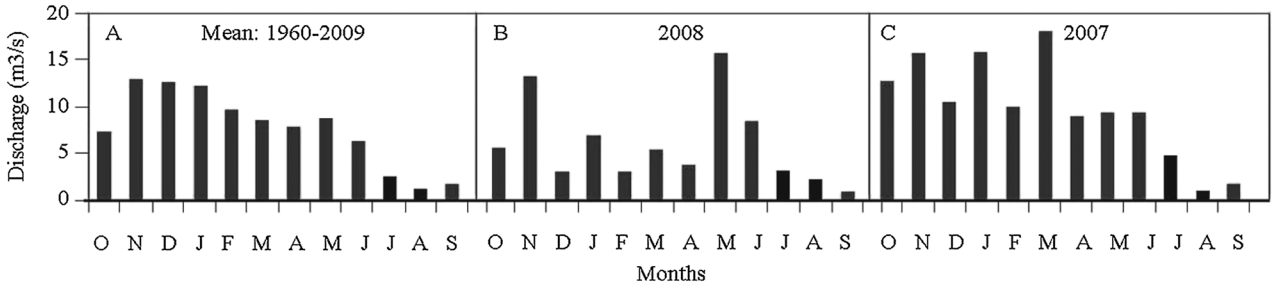

Figure 2. Tsable River water-year hydrographs. Dark bars indicate the reconstruction season (July–August). (A) Gauged mean monthly discharge over the length of record used (1960–2009); (B) mean monthly discharge in a 'more nival' year when runoff during spring snowmelt outweighed rain-derived runoff during winter; (C) mean monthly discharge in a 'more pluvial' year when runoff from winter rains outweighed runoff from spring snowmelt

streamflow' data, span the interval 1960–2009 and were normalized using a log10 transformation.

May 1 SWE records collected at the Forbidden Plateau manual snow survey site (data period February–May 1958–2014; station code 03B01; latitude: 49.653, longitude: −125.207, elevation: 1100 m asl) were retrieved from the Water Survey of Canada (http://a100.gov.bc.ca/pub/mss/stationdata.do?station=3B01). May 1 is generally the maximum annual SWE measurement in the Forbidden Plateau dataset. We estimated monthly maximum temperature and total precipitation anomaly records on the coordinates of the Tsable River hydrometric gauge site using the programme ClimateWNA, ver. 4.83 (Wang *et al.*, 2006; 2012). The programme downscales PRISM (Daly *et al.,* 2002) monthly data (2.5 × 2.5 arc min) based on the reference period 1961–1990. We compared the gauged and reconstructed streamflow records with NOAA Multivariate ENSO Index ranks (http://www.esrl.noaa.gov/psd/enso/mei/) and standardized values of the PDO index downloaded from the NOAA Earth System Research Laboratory website (http://www.esrl.noaa.gov/psd/data/climate indices/list/). Winter (averaged October–March) PDO data were used because year-to-year variability in the index is most energetic during those months (Mantua, 2002).

Tree-ring data

Mountain hemlock and amabilis fir TR width data were used for this study. In the northwestern United States and Canada, the annual radial growth of high-elevation conifer trees is often energy limited as a result of variations in snowpack depth (Peterson and Peterson, 1994). Snow may control the timing of the start or end of the growing season and, therefore, total growing season length through its influence on soil temperatures, which warm rapidly after snowmelt (Graumlich and Brubaker 1986). This climate-radial tree growth relationship is well-documented in mountain hemlock trees (Graumlich and Brubaker, 1986; Smith and Laroque, 1998; Laroque and Smith, 1999; Gedalof and Smith, 2001a; Peterson and Peterson, 2001; Zhang and Hebda, 2004; Marcinkowski *et al.*, In press) and field observations suggest amabilis fir trees typically initiate leaf and shoot expansion shortly after snowmelt (Worrall, 1983; Hansen-Bristow, 1986).

TR width data was compiled for one amabilis fir stand and eight mountain hemlock stands located on central and northern Vancouver Island (Figure 1, Table I). These data were selected because they provided the longest potentially SWE-sensitive TR width records. Crossdated amabilis fir TR width measurements collected by R. Parish at Mt. Cain in 1999 were acquired from the International Tree-Ring Data Bank website (http://www.ncdc.noaa.gov/data-access/paleoclimatology-data/datasets/tree-ring). Mountain hemlock samples were collected between 1996 and 1998 by removing two cores with a 5.0-mm increment borer from trees at standard breast height. Ring widths were measured using WinDENDRO Ver 6.1b (WinDENDRO, 1996; Laroque, 2002). In 2014, the measurements were crossdated visually (list method) and statistically verified using the programme COFECHA 3.0 (Holmes, 1983; Grissino-Mayer, 2001). In some cases physical samples were missing from the archived collections. Because crossdating was not possible without physical specimens, only a subset of the original samples could be used for each site. As a result, sample sizes per site were very low in some cases (Table I).

Tree-ring chronologies were developed using the R package dplR (Bunn, 2008). We removed long-term biological growth trend from the TR data by fitting a 100-year cubic smoothing spline with a frequency cutoff of 50 to each TR series (Cook and Peters, 1981). Dimensionless growth indices were produced by dividing ring-width measurements by the expected value of the spline. The majority of the TR data exhibited low-order autocorrelation as a result of the lagged influenced of environmental conditions in previous years (Fritts, 1976). We fit an autoregressive model to the data to remove persistence, with the model order defined by minimization of the Akaike Information Criterion. Only residual

Table I. Tree-ring chronology information. Chronologies in bold font were entered as candidate predictors in the forward stepwise model

Chronology	#	Lat/Long	Elev (m asl)	RBAR[c]	Length (years)	Series (#)	Trees (#)	r_1[d]
Bulldog Ridge[a]	1	50.28 −127.24	1010	0.22	1845–1997	9	6	0.72
Castle Mountain[a]	2	50.45 −127.12	1150	0.32	1845–1997	10	7	0.75
Colonial Creek[a]	3	50.28 −127.46	990	0.29	1940–1997	7	5	0.76
Silver Spoon[a]	4	49.98 −126.67	1100	0.37	1955–1996	11	8	0.66
N. Isl. Regional[a]		**—**	**—**	**0.26**	**1630–1997**	**37**	**28**	**0.72**
Mt. Apps[a]	5	49.44 −124.96	1340	0.29	1795–1996	40	22	0.63
Mt. Arrowsmith[a]	6	49.24 −124.59	1460	0.33	1575–1997	11	8	0.72
Mt. Washington[a]	7	49.75 −125.30	1470	0.42	1795–1996	15	12	0.68
Cream Lake[a]	8	49.48 −125.53	1340	0.36	1525–1995	29	18	0.68
C. Isl. Regional[a]		**—**	**—**	**0.30**	**1510–1997**	**95**	**61**	**0.68**
Mt. Cain[b]	**9**	**50.22 −126.35**	**1005**	**0.31**	**1520–1999**	**64**	**34**	**0.83**

[a] Mountain hemlock.
[b] Amabilis fir.
[c] Mean correlation coefficient among TR series, calculated from the detrended residual chronology.
[d] Mean first-order autocorrelation calculated using programme COFECHA, prior to autoregressive modelling.

chronologies estimated by this procedure were used in the subsequent analysis (Cook and Holmes, 1986). Series were combined into single representative 'site-level' chronologies using a bi-weight robust mean estimation (Mosteller and Tukey, 1977). Where two or more series were included from one tree, we averaged them prior to mean chronology estimation in order to weight individual trees equally. We determined the adequacy of the sample size for capturing the hypothetical population growth signal by calculating the expressed population signal (EPS; Wigley *et al.*, 1984), and truncated the chronologies where $EPS < 0.80$. Because of the low number of samples per site, we aggregated the records into regional chronologies where site-level chronologies were significantly intercorrelated. This significantly extended the lengths of our TR records by enhancing signal-to-noise ratios in the early part of the record. The methods used to estimate site-level chronologies were also used to estimate regional chronologies.

The Pearson correlation coefficient was used to summarize the strength of linear relationships between various time series in this study. All tests of association were conducted over the longest common interval between datasets. We used correlation tests to determine whether the site-level and regional TR chronologies were significantly linearly correlated with the gauged summer streamflow data, with Bonferroni corrections applied for repeated testing (Dunn 1961). The temporal stability of relationships in non-overlapping data subperiods was tested using a difference-of-correlations test that employs a Fisher's Z transformation of correlations (Snedecor and Cochran, 1989). Long chronologies that were significantly ($p < 0.01$) correlated with summer streamflow over the full length of the streamflow record were retained as candidate model predictors.

Hydroclimate relationships

To determine the climatic variables controlling summer discharge in Tsable River, and to justify a SWE-based reconstruction model of the river, we tested correlations of the gauged summer streamflow data with various monthly and seasonal climate data records. Effective sample sizes (Dawdy and Matalas, 1964) were used as needed in testing the correlations for significance, to adjust for persistence in the individual time series.

To assess the influence of snow on runoff, we tested the correlation of gauged summer streamflow data with current and previous year May 1 SWE values. We applied the previously described difference-of-correlations test (Snedecor and Cochran, 1989) to determine if there is a significant change in the relationship between streamflow and SWE before and after the 1976/77 PDO shift (Mantua, 2002). Because high summer streamflow is usually associated with enhanced snowmelt in hybrid streams (Eaton and Moore, 2010), we checked that low summer streamflow years are also influenced by meltwater by sorting the gauged summer streamflow data into lowest, middle, and highest terciles, and calculating Pearson's correlations between the summer streamflow and May 1 SWE values within each tercile.

Correlations of gauged summer runoff with monthly and seasonally aggregated temperature and precipitation data were calculated using the programme Seascorr (Meko *et al.,* 2011). Seascorr estimates confidence intervals on the sample correlations and partial correlations by a Monte Carlo simulation of the flow data by exact simulation (Meko *et al.*, 2011). Correlations of the gauged summer streamflow data with maximum temperature data were tested in 1- to 6-month intervals, with

intervals ending in each month of the 14-month period beginning in July of the previous year and ending in August of the current year. Partial correlations were then calculated to determine if annual, and especially summer, precipitation makes a significant contribution to summer runoff that is independent of the temperature influence. We also tested monthly and seasonal correlations between the temperature and precipitation data in the same seasonal and monthly groupings. Relationships to climate in the previous year were evaluated because we were curious whether they influence current-year summer runoff as a result of hydrological lag effects in the groundwater system.

Model estimation

The reconstruction model was estimated by forward stepwise multiple linear regression of the summer streamflow data in year t on the pool of candidate predictor variables in years t, $t+1$, and $t+2$. Lagged predictors were entered to allow TR information in subsequent years to inform on climate conditions in the given year (Cook and Kairiūkštis, 1990). We evaluated regression models based on a suite of statistics widely used to evaluate tree-ring based environmental reconstructions. The adjusted R^2 statistic provides a measure of the explanatory power of the models accounting for lost degrees of freedom. Analysis of the model residuals, and the Durbin–Watson (D–W) and variance inflation factor (VIF) statistics, were used to check the model fit and assumptions. The F-ratio gives an estimate of the statistical significance of the regression equation and the standard error of the estimate (SE) a measure of uncertainty of the predicted values of the model calibration. We used leave-one-out (LOO) cross-validation (Michaelsen, 1987) to validate the models against data that were not used in the calibration. This approach allowed us to use the full 37 years of corresponding streamflow and TR data for the validation procedure, which was important given the relatively short calibration interval. We calculated cross-validation statistics by comparing the predictand gauged summer streamflow data with the LOO-estimated values of the predictand. The reduction of error (RE; Fritts *et al.*, 1990) provides a rigorous measure of model skill, with a positive value indicating that the LOO estimates better predict instrumental flow data than the mean of the instrumental data. The root mean square error of cross-validation ($RMSE_v$) gives a measure of the uncertainty of the predicted values over the verification period. The Pearson correlation (r) and R^2 of the observed and LOO-estimated values provide additional measures of accuracy (Cook and Kairiūkštis, 1990). The best model was calibrated over the full instrumental streamflow data record and used to reconstruct historical summer streamflow over the length of the shortest predictor dataset. We back-transformed the reconstructed values (modelled from TRs) to the original flow units for plotting and analysis, and checked that the selected model predictors are linearly correlated with the reconstructed flow data over the full instrumental data interval. To confirm that they operate as proxies for climate in our paleohydrological model we tested whether the model predictors are correlated with May 1 SWE and/or spring/summer maximum temperature. Correlations with temperature were calculated with Seascorr using the procedure described for hydroclimate correlations.

Analysis of the reconstruction

We compared statistical properties of the reconstructed record in the separate pre-instrumental (1520–1959) and instrumental (1960–1997) periods, with those of the gauged summer streamflow data. This comparison allowed us to determine if the pre-instrumental reconstructed record differs from reconstructed record during the instrumental era in any significant way, and also allowed us to assess the capacity of our model to approximate statistical characteristics of actual Tsable River summer streamflow. Extreme single-year droughts were defined based on a bottom fifth percentile threshold of summer streamflow, calculated based on the full reconstruction data period (1520–1997). Drought timing and magnitudes were then plotted as departures from the reconstructed mean summer streamflow calculated from the instrumental period. Comparing reconstructed values in the pre-instrumental and instrumental periods puts extreme historical droughts in the context of recent conditions without making unequal comparisons between TR-modelled streamflow data and gauged streamflow data.

We calculated the return interval of extreme droughts following the equation of Mays (2005) and used Chi-squared analysis to test if the frequency of these events in the gauged summer streamflow record (1960–2009) differed from an expected frequency of five events per 100 years (bottom fifth percentile). High year-to-year summer discharge variance is typical in hybrid watersheds and can make it difficult to identify multi-year stretches of generally low runoff, so we assessed the number of years of below median runoff over a sliding 21- year window. To determine whether reduced summer runoff corresponds with enhanced overall runoff variance, we visually compared extreme drought timing and intervals of generally low discharge with a sliding 21-year average of the standard deviations of the reconstructed summer streamflow values.

The gauged and reconstructed summer streamflow records were compared with instrumental ENSO and PDO records to investigate the influence of large-scale climate modes on droughts and wet episodes. A test of proportions (Newcombe, 1998) was used to determine if the proportion of years with below-median (or above-median) runoff during El Niño years equals the proportion of years with below-median (or above-median) runoff during weak- and non-El Niño years. The strength of El Niño/La Niña in a given year was based on NOAA Multivariate ENSO Index ranks. The same difference-of-correlations test (Snedecor and Cochran, 1989) was used to determine if correlations of the winter PDO data with the gauged and reconstructed streamflow records are significantly different during cool *versus* warm PDO phases. Effective sample sizes (Dawdy and Matalas, 1964) were used as needed to account for autocorrelation in the individual time series. A Morlet wavelet analysis (Torrence and Compo, 1998) was performed on the full reconstructed record to highlight localized fluctuations of power over time that may be associated with climate modes.

RESULTS

Tree-ring data

We developed eight site-level mountain hemlock chronologies and one site-level amabilis fir chronology for this study (Table I). Four significantly intercorrelated (mean $r = 0.753$, $p < 0.01$) mountain hemlock chronologies were combined into a regional chronology representing northern Vancouver Island, and four significantly intercorrelated (mean $r = 0.841$, $p < 0.01$) mountain hemlock chronologies were combined into a regional chronology representing the central part of Vancouver Island. Consolidating short site-level chronologies enhanced chronology sample depths to the extent that the regional chronologies could be used for dendroclimatic reconstruction. Chronology lengths for the final chronologies ranged from 367 to 487 years and mean correlation coefficient among TR series (RBAR) ranged from $r = 0.26$ to 0.31 (Table I). All chronologies were significantly ($p < 0.01$) correlated with the gauged summer streamflow data (r ranging from 0.466 to 0.867). The two regional chronologies and the Mount Cain amabilis fir chronology were retained as candidate model predictors.

Hydroclimate relationships

Of the monthly and seasonal climate data tested, the Tsable River gauged summer streamflow data are most strongly correlated with current-year May 1 SWE (Table II), a positive relationship that is stable over the over the 1976/1977 PDO shift (Mantua, 2002). This relationship is also significant ($p < 0.05$) in the lower and upper, but not middle, terciles of the gauged data (lower tercile: $n = 17$, $r = 0.529$, upper tercile: $n = 17$, $r = 0.552$). The gauged data are also negatively correlated with maximum temperature in March through August of the current year (Table II, Figure 3) and, independently, with winter precipitation but not summer precipitation (Figure 3). No relationships to climate in the previous year were significant. Panel B in Figure 3 indicates that temperature and precipitation data are significantly negatively correlated in July through October and May through August.

Model estimation and reconstruction

A reconstruction that used the central island regional chronology in time t and Mt. Cain amabilis fir chronology in time t was selected as the best model

$$Q = 2.05 - (0.993 * central\ island\ TRs) - (0.527 * Mt.\ Cain\ TRs)$$

Time plots of the chronologies are presented in Figure 4. Despite similarities between the predictors, the standardized coefficients indicate that the amabilis fir chronology contributes significant additional explanatory power to the model (beta = −0.33) relative to the central island chronology (beta = −0.60). The reconstructed record spans 1520–1997 and explains 63% of the variance in the gauged Tsable River summer streamflow data (1960–2009) accounting for lost degrees of freedom. The reconstructed and the gauged streamflow data are compared in original streamflow units in Figure 5A. Regression and cross-validation statistics are summarized in Table III, and a time plot of

Table II. Hydroclimate correlations

	Central Isl. TM	Mt. Cain AA	SWE	Max T
Q (JA)	−0.75	−0.61	May 0.70	Mar–Aug −0.61
Central Isl. TM	—	0.46	May −0.58	Mar–Apr 0.41
Mt. Cain AA		—	May −0.53	Jul–Aug −0.36

Current year in capital letters.
For all correlations $p < 0.01$.

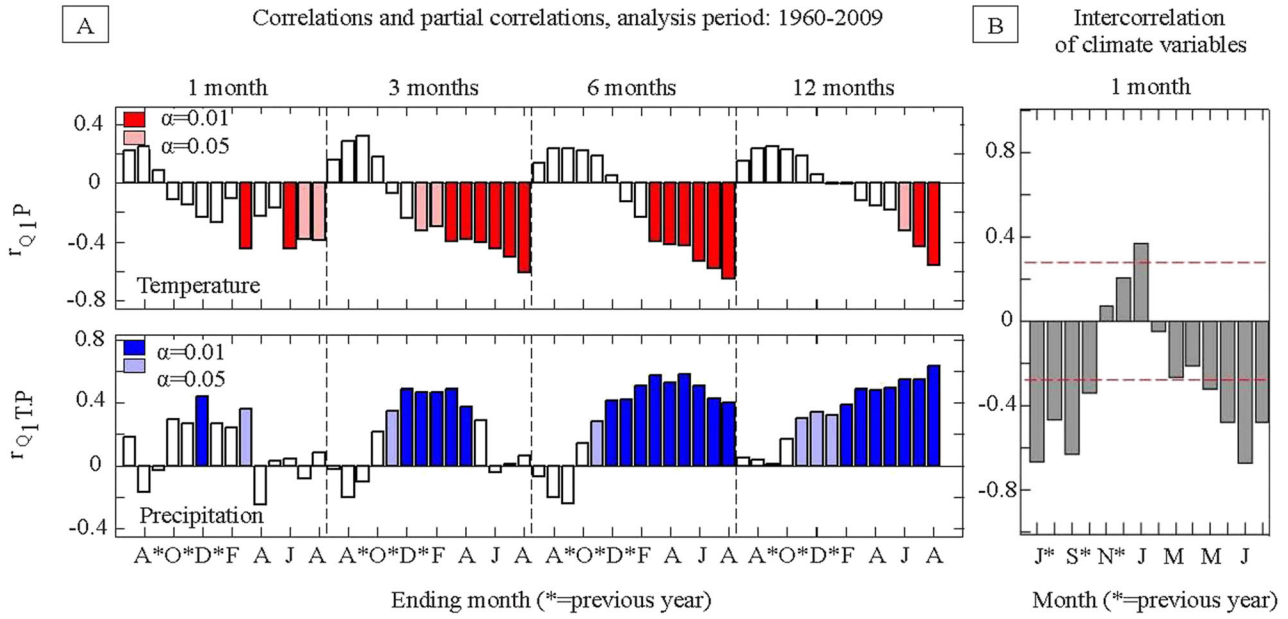

Figure 3. (A) Monthly and seasonal correlations between Tsable River July–August streamflow (Q) and maximum temperature, over 1-, 3-, 6-, and 12-month sliding windows beginning in the previous July through current August (top), and; monthly and seasonal partial correlations between Tsable River flows and precipitation, controlling for the influence of maximum temperature. (B) Monthly correlations between temperature and precipitation, beginning in the previous July through current August. Red-hatched bands represent 95% confidence intervals with the confidence interval set at $0 + 1.96/\sqrt{N}$, where N is the sample size. All tests were calculated using Seascorr

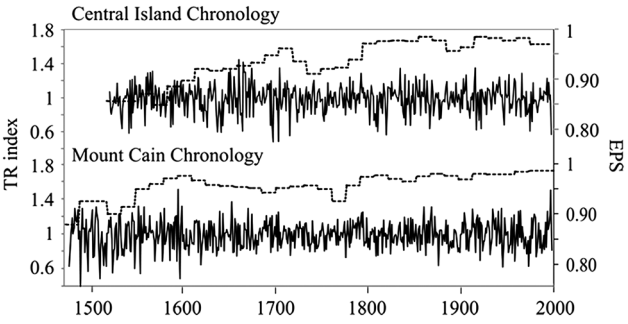

Figure 4. Time plot of tree-ring chronologies used as model predictors. EPS values are plotted with a hatched line

the cross validation is presented in Figure 5B. Collinearity diagnostics indicate that predictors are adequately independent, and the F-ratio indicates a statistically significant regression equation. The positive RE value is very similar to the validation R^2, and the SE value approximates that of the $RMSE_v$, suggesting a well-validated model. The LOO-generated predicted values of the predictand are significantly and strongly ($r = 0.62$, $p < 0.01$) correlated with the gauged summer streamflow data. Analysis of regression residuals indicated that the models do not violate regression assumptions. The chronologies are significantly ($p < 0.01$) correlated with the gauged summer streamflow data over the full period of that record (Figure 5C, Table II).

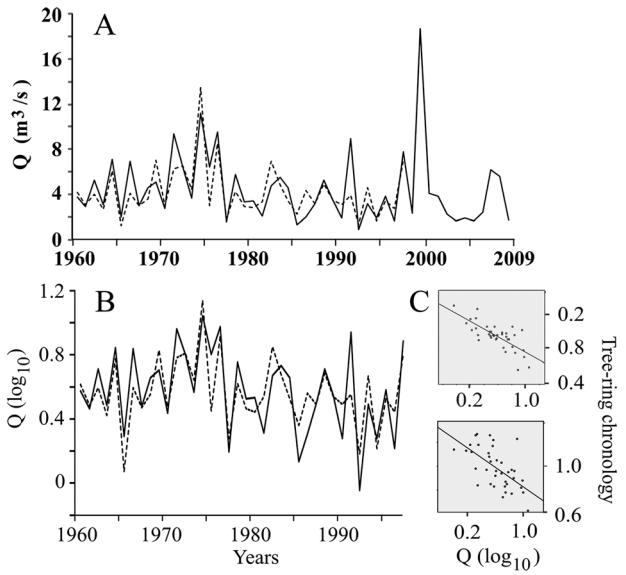

Figure 5. (A) Time plot of the reconstructed (hatched line) and gauged (solid line) summer streamflow data, backtransformed to original flow units, over the model calibration period. The instrumental data extend to 2009. (B) Time plot of the cross validation. The solid line represents the gauged (transformed) streamflow data, and the hatched line represents the LOO estimates. (C) Scatterplots of the linear associations of the central island regional chronology (above: $R^2 = -0.565$) and the Mount Cain chronology (below: $R^2 = -0.373$) with the predictand streamflow data

The central island regional chronology is most strongly negatively correlated with May 1 SWE, and is also weakly positively correlated with maximum temperature

Table III. Reconstruction and cross-validation statistics

Adj. R^2	D–W	VIF	SE	F-ratio[a]	RE	$RMSE_v$[b]	r[c]	R^2[d]
0.63	2.08	1.27	0.16	32.86	0.62	0.16	0.79	0.62

[a] Significant at the 99% level.
[b] Derived from transformed flow (unitless).
[c] Cross-validation r ($p < 0.01$).
[d] Cross-validation R^2.

in March through April (Table II). The Mt. Cain amabilis fir chronology is most strongly negatively correlated with May 1 SWE, and also exhibits a weaker negative correlation with maximum temperature during July and August (Table II, Figure 4).

Analysis of the reconstruction

The cross-validation time plot exhibits strong coherence between the gauged summer streamflow data and the LOO-estimated values (Figure 5B). While the magnitudes of both high and low flows are over and underestimated at times (for example, the magnitudes of the three lowest flows are underestimated), the modelled data track the instrumental data well overall.

Generally, our reconstruction describes very high year-to-year variance typical of a small hybrid streamflow regime that shifts intermittently from more pluvial to more nival states, and where variance is not smoothed by hydrological lag over multiple years (Figure 6). Autocorrelation function plots indicate that neither the gauged or reconstructed summer streamflow data are significantly autocorrelated at lags <15 years. Generally symmetric high-to-low flow variance is punctuated by intervals of enhanced variance driven by high flows (Figure 6). While the mean summer streamflow values and standard variances are similar in the gauged and reconstructed records, the gauged minimum/maximum values are slightly lower/higher than the reconstructed values (Table IV). A scatterplot of the standardized residual values against the gauged summer streamflow data, as well as the width of the reconstruction confidence intervals (Figure 6) suggest that our model most accurately estimates summer streamflow values in low flow years and may underestimate them in high flow years.

The timing and magnitudes of bottom fifth percentile flow years ($Q < 1.67\,m^3/s$) are plotted in Figure 6. Twenty-two extreme droughts occurred prior to the instrumental record, with a 20 year return interval (Figure 6, Table V). The most extreme droughts recorded occurred in 1651, 1660, and 1665, with an unusual cluster of seven drought years occurring between 1649 and 1667. Only once in the last 440 years have drought conditions persisted for three or more years (1665–1667). None of the reconstructed droughts was more severe than the worst instrumental drought in 1992, when summer streamflow was only 21% of the reconstructed instrumental period mean discharge (Table V).

Table IV. Gauged and reconstructed streamflow statistics

Streamflow data	min (m^3/s)	mean (m^3/s)	max (m^3/s)	cv[a]	r_1[b]
Gauged	0.9	4.4	18.6	0.53	−0.11
Reconstructed (instrumental period)	1.3	4.2	13.4	0.69	−0.12
Reconstructed (pre-instrumental period)	0.7	4.1	13.3	0.54	−0.11

[a] Coefficient of variation.
[b] First-order autocorrelation coefficient. None significant ($p < 0.05$) for lags 1–15.

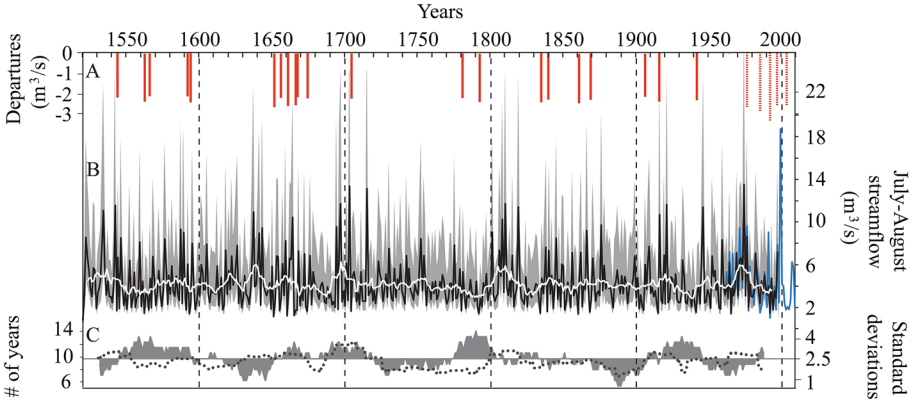

Figure 6. (A) Extreme droughts, plotted as departures from the reconstructed instrumental period mean. Reconstructed droughts are represented with red bars and gauged droughts with red hatched bars. The gauged drought magnitudes are calculated from a threshold derived from the reconstructed record. (B) Time plot of reconstructed Tsable River July–August streamflow (black line) with 5-year running mean (white line), gauged streamflow data (blue line), and 95% confidence intervals calculated from the RMSEv (Weisberg 1985; grey envelope). (C) Line graph of the number of years when July–August streamflow fell below the median value of the full-period reconstruction, plotted over a 21-year sliding window (grey fill) and a sliding 21-year average of the standard deviations of the reconstructed streamflow data (dotted line). For both the median departures and standard deviations, each plotted value represents the central value of the sliding window

Table V. Pre-instrumental bottom fifth percentile low-flow timing and magnitudes (regular font), and gauged flows falling below the reconstructed bottom fifth percentile threshold (bold font). Presented in order of severity

Year	Departure[a] (m^3/s)	Mean July–August flow (m^3/s)	% of reconstructed instrumental period mean Q
1992	**−3.33**	**0.91**	**21**
1651	−3.21	1.03	23
1660	−3.14	1.10	25
1665	−3.11	1.13	26
1860	−2.98	1.30	29
1593	−2.93	1.31	30
1792	−2.92	1.32	30
1834	−2.91	1.33	30
1915	−2.89	1.35	31
1985	**−2.86**	**1.38**	**31**
1562	−2.88	1.40	32
1941	−2.81	1.43	32
1868	−2.76	1.48	33
1839	−2.75	1.49	34
1704	−2.70	1.54	35
1674	−2.69	1.55	35
1780	−2.66	1.58	36
1543	−2.65	1.59	36
1655	−2.65	1.59	36
1977	**−2.65**	**1.59**	**36**
1666	−2.62	1.62	37
1667	−2.62	1.62	37
1905	−2.60	1.64	37
1565	−2.58	1.66	38
1591	−2.58	1.66	38
1996	**−2.58**	**1.66**	**38**
2003	**−2.58**	**1.66**	**38**

[a] Departure from the reconstructed instrumental period mean (4.24 m^3/s).

Gauged summer streamflow values also fell below the bottom fifth percentile threshold in five years (1977, 1985, 1992, 1996, and 2003; Figure 6, Table V). The Chi-squared analysis indicated that the frequency of extreme droughts in the gauged record does not differ from the expected frequency (Chi-squared = 4.69, $p = 0.10$). We have reported the magnitudes of extreme instrumental droughts in terms of their departure from the reconstruction mean over the instrumental period which is a slightly unequal comparison because the instrumental period was omitted from the calculation of the bottom fifth percentile threshold.

The number of years where summer streamflow fell below the median value of the full-period reconstruction is plotted over a 21-year sliding window in Figure 6. Each value in Figure 6 represents the central value of the sliding window. The plot makes it possible to identify periods of time when summer streamflow was either high or low overall relative to the median, despite the very high year-to-year variance dominating the reconstruction. Periods of overall lower flows occurred from the mid-1560s to late 1500s, 1650–1720, 1770–1810, and 1905–1941. Visual comparison of these periods with intervals of higher year-to-year summer streamflow variance, highlighted in Figure 6 by the sliding-mean standard deviations, does not suggest any relationship of generally higher/lower summer streamflow with higher overall variance.

Neither the gauged or reconstructed summer streamflow records exhibited differences in the number of below (above)-median flows during El Niño *versus* weak- and non-El Niño years (Table VI). Both records were significantly correlated with winter PDO over the full common data interval ($r = -0.47$ and $r = -0.23$ respectively, $p < 0.01$), although the reconstructed record exhibited a weaker relationship. Relationships with winter PDO were stronger during the early/cool phase (1960–1976; $r = -0.57$ and $r = -0.47$ respectively, $p < 0.01$) than the late/warm phase (1977–1997; $r = -0.30$ and $r = -0.11$ respectively, $p < 0.01$), but the difference between correlations in these periods was not statistically significant for either record. The wavelet power spectrum identifies repeating, but not necessarily regular, fluctuations (energy) in the time series over time (Torrence and Compo, 1998). The reconstructed streamflow data (Figure 7) exhibits significant ($p < 0.01$) energy in the approximately 2, 4, and 8-year bands that is intermittent over time, and energy in the approximately 15–30 year band that is more persistent over time, including throughout the mid- 1600s, 1800–1850, and 1960–1980.

Table VI. Test of proportions determining associations of instrumental and reconstructed flow data to El Niño events, calculated over the period 1960–1997. Calculated using function *prop.test* in R. Proportions of years in each streamflow category noted in parentheses. The null hypothesis that both groups have the same true proportions was true for all tests, with p values ranging around 0.32 (average)

Streamflow category	# El Niño years	# non-El Niño years	# El Niño and non-El Niño years
Instrumental flow data			
Below median	9 (40.9%)	10 (62.5%)	19 (50%)
Above median	13 (59.1%)	6 (37.5%)	19 (50%)
Total	22 (100%)	16 (100%)	38 (100%)
Reconstructed flow data			
Below median	8 (36.4%)	11 (68.7%)	19 (50%)
Above median	14 (63.6%)	5 (31.3%)	19 (50%)
Total	22 (100%)	16 (100%)	38 (100%)

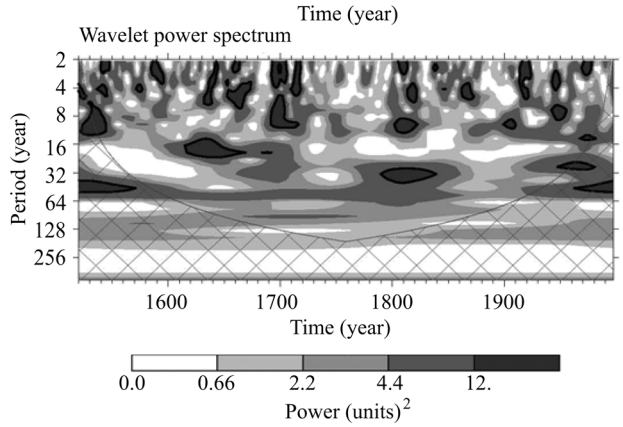

Figure 7. Morlet wavelet power spectrum on the full reconstructed streamflow record. The black contours represent the 95% confidence level based on a white-noise background spectrum. The hatched area represents areas of the spectrum susceptible to the effects of zero padding (Torrence and Compo 1998)

DISCUSSION

Reconstruction model

Our reconstruction effectively estimates July-August streamflow in Tsable River based on two TR-derived proxy records sensitive to regional-scale SWE variability. Correlation analyses indicate that runoff during this season is driven principally by snowmelt, and that the selected TR predictors primarily operate as proxies for that streamflow component in our paleohydrological model. The sensitivity of gauged summer streamflow data to previous winter SWE and spring/summer maximum temperatures supports the interpretation that Tsable River is characterized by a hybrid hydrological regime. Tercile correlations confirm that low streamflow values, not just high streamflow values, are influenced by snowmelt. The gauged streamflow record is also influenced by summer temperature fluctuations which can impact runoff because of the large relative influence of evaporation on small basins (Margolis *et al.,* 2011). Some temperature-related variability may be incorporated into the reconstruction because the two predictor TR chronologies are influenced by temperature in the spring and summer, respectively. The model residuals are correlated with maximum temperature during March (-0.42, $p < 0.01$) but not during summer months, suggesting summer temperature related variability from the Mount Cain TR chronology may influence the model estimates. The negative relationship between TRs and summer temperature means that summer temperature information within the TR chronology serves to weaken the relationship between TRs and streamflow, which may reduce model accuracy (although the TR-temperature relationship is notably weak; $r = -0.36$, $p < 0.01$). Finally, the instrumental streamflow data are influenced by winter rainfall persisting in the groundwater system, and summer rainfall. Neither of these flow components is captured by our model but, because they contribute little to summer runoff, it is not likely this seriously reduces the accuracy of the reconstruction. A possible limitation of our reconstruction is that cross-validation statistics can be biased upward when the cross-validation period is short (Meko, 2006), although the cross-validation time plot indicates a strong model validation.

Our reconstruction is primarily 'tuned' to SWE-driven runoff variations. However, we found that the gauged summer streamflow data are also influenced by spring/summer maximum temperature. The inability of our model to fully capture temperature-driven summer streamflow variability likely contributes to general underestimation of the severity of the lowest gauged flows (3/4 lowest instrumental flow values are underestimated), although low flows are still more precisely estimated than high flows. The incorporation of a summer temperature-sensitive proxy in a similar model may improve the accuracy of low-flow magnitude estimations and, given the non-independence of temperature and precipitation fluctuations during summer, might also enable a model to account for some portion of variability in summer precipitation.

As is typical in TR-based regression, our model does not capture the full range of instrumental streamflow variance (Table IV; Cook and Kairiūkštis, 1990). We emphasize that as a result, the reconstruction likely underestimates the severity of historical lowest summer flows. For example, although the model residuals suggest low flows are generally more accurately estimated than high flows, the magnitudes of the three worst instrumental droughts are all underestimated in the cross-validated and reconstructed data (Figure 5A, B). We have also reconstructed mean, not minimum, July–August streamflow values; actual lowest streamflow values would be lower than those estimated by our model.

Extreme droughts

Twenty-two extreme droughts occurred over the 439-year pre-instrumental record. As a modern analogue, the low-flow magnitudes in all but one of these years were more severe than the gauged values in 2003 and 2009 when severe summer drought throughout southern and coastal B.C. seriously impacted community, irrigation, and hydroelectric water supplies in un-glaciated catchments (B.C. Ministry of Environment, 2010; Puska *et al.,* 2011). Our reconstruction suggests that droughts of the severity of those in 2003 and 2009 are not anomalous relative to the last several hundred years and should be accounted for in water management strategies

(in fact, 2009 was not flagged as an extreme drought year based on the long-term threshold). Further, worst-case scenario natural droughts based on hydrometric data records are likely underestimated because more severe events occurred outside the hydrometric data period. It is possible that extreme natural low flows, paired with pressures from land-use and climate change, could result in a drought that is more severe than any since 1520. It is important to consider that very low flows in unglaciated Vancouver Island streams since 2009, especially in 2014 and 2015 (B.C. Ministry of Forests, Lands and Natural Resource Operations 2014; B.C. River Forecast Centre, 2015), may well have surpassed the severity of gauged droughts analysed for this study but could not be accounted for because of unavailable hydrometric data. The instrumental drought in 1992 may be more extreme than any in the reconstructed record, but this should be interpreted conservatively because the reconstructed streamflow variance is somewhat suppressed relative to the gauged record; actual magnitudes of pre-instrumental low flows may be as or more extreme than in 1992.

Our results suggest that relative to the preceding 440 years, the magnitudes of extreme droughts in Tsable River did not generally worsen from 1960 to 2009. Frequencies of lowest flow events also did not increase. A large outlier (high-flow year) in 1999 obscures a significant long-term negative trend in the gauged data (tested using a *t*-test of the slope of a regression of the instrumental flow data on time with 1999 removed) indicating that, with the exception of one year, Tsable River summer runoff has declined overall between 1960 and 2009. Analysis of SWE and precipitation data shows the outlier is related to very high snowfall (July–August precipitation was equal to the long-term 1960–2009 average in that year, while SWE was 217% of the average). This trend is not exceptional compared to the rest of the reconstruction, which suggests long-term streamflow declines of similar length and magnitude began around 1640, 1700, and 1800. Without data for the most extreme recent drought years, it is not possible to assess the unusualness of recent streamflow trends relative to the last few centuries.

Our findings highlight that consecutive years of very low flows have been extremely rare in the Tsable River system, which is consistent with minimal multi-year hydrological lag in small coastal watersheds and is an important hydrological feature for water management. Because the likelihood of extreme droughts is largely unrelated to conditions in the previous year, these events are highly unpredictable compared with large basins where persistent, multi-year drought is typical (Meko and Woodhouse, 2010). From a model-development standpoint, mimicking the zero-autocorrelation structure of the gauged summer streamflow data was critical for developing an accurate reconstruction. The dendrohydrological approach risked introducing 'artificial' persistence related to biological tree growth into our model, but use of residual chronologies guarded against this.

We found no evidence that the timing of below- or above- median streamflow in Tsable River corresponds with El Niño or weak- and non-El Niño years, in either the instrumental or reconstructed flow data. We evaluated El Niño years because they are typically associated with the low flows of interest to this study and which are most accurately estimated by our model. We did not evaluate associations with La Niña events that are typically more strongly associated with annual streamflow in hybrid watersheds, and correspond with enhanced winter precipitation and total runoff (Fleming *et al.,* 2007). In contrast, both the reconstructed and gauged streamflow records are influenced by winter PDO during the common data interval, with the strongest (negative) relationships occurring during the cool phase of the oscillation. This suggests an influence of SWE on summer low flows, consistent with cool PDO phases promoting more snow and higher snowmelt-derived runoff than warm phases (Fleming *et al.,* 2007). That the difference in correlations between the warm and cool phases was not statistically significant may have been because of small effective sample sizes (17 and 21 years). Intermittent ENSO-like power in the reconstructed record is evident in the approximately 2, 4, and 8-year bands of the wavelet power spectrum (Figure 7). PDO-like multidecadal power weakens between 1850 and 1910, as documented in other independent reconstructions of that oscillation (Gedalof and Smith, 2001b, MacDonald and Case, 2005).

Comparison with historical temperature, precipitation, and drought records is made difficult by a lack of relevant high-resolution records in Pacific Canada and the northwestern United States. The most pertinent records, which represent seasonal and/or spatial contexts distinct from those of this study, unsurprisingly yielded no notable similarities to historical Tsable River streamflow variability (Graumlich and Brubaker 1986; Larocque and Smith 2005; Luckman and Wilson 2005; Jarrett 2008; Wiles *et al*., 2014). Neither does our reconstruction correspond with the few (non-hybrid) streamflow reconstructions developed in B.C. (Gedalof *et al*., 2004, Hart *et al*., 2010, Starheim *et al*., 2013), similar records from Canada's western interior (Case and MacDonald 2003; Axelson *et al*., 2009), or large-scale historical drought episodes such as the 1929–1940 Dust Dowl, the 1946–1956 drought in the southwestern United States (Fye *et al.,* 2003), or the 16th century megadrought (Stahle *et al.,* 2000). In the instrumental

period, recent large-scale droughts in the Canadian Prairie provinces (e.g. 2002; 1999–2005; Canadian Foundation for Climate and Atmospheric Sciences 2010) are not expressed in the Tsable River gauged record, reinforcing the distinct hydroclimatological character of B.C.'s small coastal basins relative to surrounding regions.

CONCLUSION

Long-term perspectives on hydroclimate variability are critical for water management, with small temperate watersheds representing a frontier for paleohydrological modelling (Biondi and Strachan, 2012). We demonstrate that a dendrohydrological approach focused on the SWE-driven streamflow component is appropriate for determining drought-season runoff in small hybrid watersheds in coastal B.C. Tree-ring width records that are energy-limited by spring snowmelt timing were effective proxies for this streamflow component. Our reconstruction of Tsable River suggests that the severity of droughts in the 440 years preceding the instrumental record exceeded modern analogues such as the 2003 and 2009 droughts. The fact that recent 'extreme' events fall within a natural range of multi-century variability means that rather than being considered anomalies, extreme droughts should be expected and incorporated into drought management strategies. Most importantly, our findings suggest that worst-case scenario natural drought estimates based on hydrometric data are likely underestimated. Given projected climate trends and pressures from land-use change and increasing human demand for water in the study area, exacerbation of natural droughts can be reasonably anticipated in hybrid basins in coming decades, potentially resulting in low flows that exceed any since 1520.

There has been a significant decline in Tsable River summer runoff from 1960 to 2009 with the exception of one year. The frequency of extreme droughts did not increase between 1960 and 2009, but we could not account for severe events after 2009 — including the major droughts that occurred in 2014 and 2015 — because of a lack of hydrometric data. Both the gauged and reconstructed streamflow records experienced significantly greater runoff during cool phases of the PDO, which favour deep snowpacks. There was no measurable influence of El Niño on the timing of below-median flows but ENSO-type variability is apparent in the wavelet analysis. This variability may be related to the influence of La Niña on high flows in hybrid systems in the study area. While our reconstruction is primarily 'tuned' to SWE-related flow variability, a model that could account for the influence of spring/summer temperature on summer streamflow may improve drought magnitude estimates.

ACKNOWLEDGEMENTS

Funding for this project was provided by the Natural Sciences and Engineering Research Council of Canada (NSERC) awards to Coulthard (Alexander Graham Bell Canada Graduate Scholarship CGS-D, Michael Smith Foreign Study Supplement) and an NSERC Discovery Grant awarded to Smith. The authors wish to thank Dave Meko, Malcolm Hughes, and Dan Griffin for their comments on the ideas presented, and the Laboratory of Tree-Ring Research at the University of Arizona for hosting Coulthard in Spring 2014. We also wish to acknowledge the data collection efforts of Laroque and Parish.

REFERENCES

Axelson JN, Sauchyn DJ, Barichivich J. 2009. New reconstructions of streamflow variability in the South Saskatchewan River Basin from a network of tree ring chronologies, Alberta Canada. *Water Resources Research*. DOI:10.1029/2008WR007639.

B.C. Conservation Foundation. 2006. Vancouver Island Focus Watersheds: Trent and Tsable rivers. Retrieved from http://www.bccf.com/steelhead/focus5.htm

B.C. Ministry of Environment, Water Protection and Sustainability Branch. 2013. *A Water Sustainability Act for B.C.: legislative proposal overview*. Retrieved from http:// engage.gov.bc.ca/watersustainabilityact/files/2013/10/WSA_overview_web.pdf

B.C. Ministry of Environment. 2010. Preparing for Climate Change: British Columbia's Adaptation Strategy. Retrieved from http://www2.gov.bc.ca/gov/DownloadAsset?assetId=29CDF35B126E483A966B0D5DAE2E3E38&filename=adaptation_strategy.pdf

B.C. Ministry of Forests, Lands and Natural Resource Operations. 2014. Water Supply and Streamflow Conditions Bulletin. Retrieved from http://bcrfc.env.gov.bc. ca/bulletins/watersupply/index-watersupply.htm

B.C. River Forecast Centre. 2015. Snow Survey and Water Supply Bulletin. Retrieved June 20, 2015, from http://bcrfc.env.gov.bc.ca/bulletins/watersupply/current.htm

Beaulieu M, Schreier H, Jost G. 2012. A shifting hydrological regime: a field investigation of snowmelt runoff processes and their connection to summer base flow, Sunshine Coast, British Columbia. *Hydrological Processes* **26**(17): 2672–2682.

Biondi F, Strachan S. 2012. Dendrohydrology in 2050: challenges and opportunities. *Toward a Sustainable Water Future: Visions for* **2050**: 355–362.

Boninsegna A, Argolla J, Aravena J-C, Barichivich J, Christie D, Ferrera ME, Lara A, Le Quesne C, Luckman BH, Masiokas MH, Morales MS, Oliviera JM, Roig F, Srur A, Villalba R. 2009. Dendroclimatological reconstructions in South America: a review. *Palaeogeography, Palaeoclimatology, Palaeoecology* **281**(3–4): 210–228.

Bunn AG. 2008. A dendrochronology program library in R (dplR). *Dendrochronologia* **26**(2): 115–124.

Canadian Foundation for Climate and Atmospheric Sciences. 2010. Annual Progress Report for the Drought Research Initiative (DRI). Retrieved from http://www.drinetwork.ca/pdf/2009_DRI_Annual_Report.pdf.

Case RA, MacDonald GM. 2003. Tree ring reconstructions of streamflow for three Canadian prairie rivers. *JAWRA Journal of the American Water Resources Association* **39**(3): 703–716.

Cook ER, Holmes RL. 1986. *Users Manual for Program ARSTAN*. Laboratory of Tree-Ring Research, University of Arizona: Tucson, USA.

Cook E, Kairiūkštis L (Eds). 1990. *Methods of Dendrochronology: Applications in the Environmental Sciences*. Kluwer Aacademic Publishers: Netherlands.

Cook ER, Peters K. 1981. The smoothing spline: a new approach to standardizing forest interior tree-ring width series for dendroclimatic studies. *Tree-Ring Bulletin* **41**(1): 45–53.

Daly C, Gibson WP, Taylor GH, Johnson GL, Pasteris P. 2002. A knowledge-based approach to the statistical mapping of climate. *Climate Research* **22**(2): 99–113.

Dawdy D, Matalas N. 1964. Statistical and probability analysis of hydrologic data, part III: Analysis of variance, covariance and time series. In *Handbook of Applied Hydrology, A Compendium of Water-Resources Technology*, Chow VT (ed). McGraw-Hill: New York, NY; 8.68–8.90.

Dunn OJ. 1961. Multiple comparisons among means. *Journal of the American Statistical Association* **56**(293): 52–64.

Eaton B, Moore R. 2010. Regional hydrology. In *Compendium of Forest Hydrology and Geomorphology in British Columbia*, Pike RG, Redding TE, Moore RD, Winkler RD, Bladon KD (eds). Victoria, BC: Ministry of Forests and Range Research Branch / FORREX Forest Research Extension Partnership; 85–110.

Fleming SW, Whitfield PH, Moore RD, Quilty EJ. 2007. Regime-dependent streamflow sensitivities to Pacific climate modes cross the Georgia–Puget transboundary ecoregion. *Hydrological Processes* **21** (24): 3264–3287.

Fritts HC. 1976. *Tree Rings and Climate*. UK. Academic Press: London.

Fritts HC, Guiot J, Gordon GA. 1990. Verification. In *Methods of Dendrochronology: Applications in the Environmental Sciences*, Cook ER, Kairiūkštis L (eds). Kluwer Aacademic Publishers: Netherlands; 178–184.

Fye FK, Stahle DW, Cook ER. 2003. Paleoclimatic analogs to twentieth-century moisture regimes across the United States. *Bulletin of the American Meteorological Society* **84**(7): 901–909.

Gedalof Z, Smith DJ. 2001a. Dendroclimatic response of mountain hemlock (*Tsuga mertensiana*) in Pacific North America. *Canadian Journal of Forest Research* **31**(2): 322–332.

Gedalof Z, Smith DJ. 2001b. Interdecadal climate variability and regime-scale shifts in Pacific North America. *Geophysical Research Letters* **28** (8): 1515–1518.

Gedalof Z, Peterson D, Mantua N. 2004. Columbia river flow and drought since 1750. *JAWRA Journal of the American Water Resources Association* **40**(6): 1579–1592.

Graumlich L, Brubaker L. 1986. Reconstruction of annual temperature (1590–1979) for Longmire, Washington, derived from tree rings. *Quaternary Research* **25**(2): 223–234.

Grissino-Mayer HD. 2001. Research report evaluating crossdating accuracy: a manual and tutorial for the computer program COFECHA. *Tree-Ring Research* **57**(1): 115–124.

Hansen-Bristow K. 1986. Influence of increasing elevation on growth characteristics at timberline. *Canadian Journal of Botany* **64**(11): 2517–2523.

Hart SJ, Smith DJ, Clague JJ. 2010. A multi-species dendroclimatic reconstruction of Chilko River streamflow, British Columbia, Canada. *Hydrological Processes* **24**(19): 2752–2761.

Holmes RL. 1983. Computer-assisted quality control in tree-ring dating and measurement. *Tree-Ring Bulletin* **43**(1): 69–78.

Jarrett P. 2008. *A Dendroclimatic Investigation of Moisture Variability and Drought in the Greater Victoria Water Supply Area, Vancouver Island, British Columbia*. Unpublished MSc. thesis, University of Victoria: Victoria B.C., Canada.

Kiffney P, Bull J, Feller M. 2002. Climatic and hydrologic variability in a coastal watershed of southwestern British Columbia. *JAWRA Journal of the American Water Resources Association* **38**(5): 1437–1451.

Klinka K, Pojar J, Meidinger D. 1991. Revision of biogeoclimatic units of coastal British Columbia. *Northwest Science* **65**(1): 32–47.

Larocque SJ, Smith DJ. 2005. A dendroclimatological reconstruction of climate since AD 1700 in the Mt. Waddington area, British Columbia Coast Mountains. *Canada. Dendrochronologia* **22**(2): 93–106.

Laroque CP. 2002. *Dendroclimatic Response of High-Elevation Conifers, Vancouver Island, British Columbia (Doctoral Dissertation)*. University of Victoria: Victoria, BC.

Laroque CP, Smith DJ. 1999. Tree-ring analysis of yellow cedar (*Chamaecyparis nootkatensis*) on Vancouver Island British Columbia. *Canadian Journal of Forest Research* **29**(1): 115–123.

Lill A. 2002. Greater Georgia Basin steelhead recovery action plan. Report prepared for BC Conservation Foundation: Greater Georgia Basin Steelhead Recovery Plan, Nanaimo, BC. Retrieved from http://www.bccf.com/steelhead /pdf/Steelheadreport092702.pdf

Loaiciga H, Haston A, Michaelsen J. 1993. Dendrohydrology and long-term hydrologic phenomena. *Reviews of Geophysics* **31**(2): 151–171.

Luckman BH, Wilson RJS. 2005. Summer temperatures in the Canadian Rockies during the last millennium: a revised record. *Climate Dynamics* **24**(2–3): 131–144.

MacDonald GM, Case RA. 2005. Variations in the Pacific Decadal Oscillation over the past millennium. *Geophysical Research Letters* **L08**: 703. DOI:10.1029/2005GL022478.

Mantua N. 2002. Pacific-Decadal Oscillation. In MacCracken M, Perry JS. *Encyclopedia of Global Environmental Change*. **1**: 592–594 (Eds). John Wiley and Sons: Chichester: UK.

Mantua N, Tohver I, Hamlet A. 2010. Climate change impacts on streamflow extremes and summertime stream temperature and their possible consequences for freshwater salmon habitat in Washington State. *Climatic Change* **102**(1–2): 187–223.

Marcinkowski K, Peterson DL, Ettl GJ. In press. Nonstationary Temporal Response of Mountain Hemlock Growth to Climatic Variability in the North Cascade Range. *Canadian Journal of Forest Research*. In press. DOI: 10.1139/cjfr-2014-0231

Margolis E, Meko D, Touchan R. 2011. A tree-ring reconstruction of streamflow in the Santa Fe River, New Mexico. *Journal of Hydrology* **397**(1): 118–127.

Mays LM. 2005. *Water Resources Engineering*. Wiley & Sons: New York, NY.

Meko DM. 2006. Tree-ring inferences on water-level fluctuations of Lake Athabasca. *Canadian Water Resources Journal* **31**(4): 229–248.

Meko D, Woodhouse C. 2010. Application of streamflow reconstruction to water resources management. In *Dendroclimatology*, Hughes MK, Swetnam TW, Diaz HF (eds). Springer: Netherlands; 231–261.

Meko D, Touchan R, Anchukaitis K. 2011. Seascorr: a MATLAB program for identifying the seasonal climate signal in an annual tree-ring time series. *Computers & Geosciences* **37**(9): 1234–1241.

Michaelsen J. 1987. Cross validation in statistical climate forecast models. *Journal of Applied Meteorology* **26**(11): 1589–1600.

Moore RD, Allen DM, Stahl K. 2007. Climate change and low flows: influences of groundwater and glaciers. Final report prepared for Climate Change Action Fund, Natural Resources Canada, Vancouver, BC. Retrieved from https://www.sfu.ca/personal/ dallen/ CCAF_ A875-FinalReport.pdf

Mosteller F, Tukey J. 1977. *Data Analysis and Regression: a Second Course in Statistics*. Addison-Wesley Publishing Company: Reading, MA.

Newcombe RG. 1998. Interval estimation for the difference between independent proportions: comparison of eleven methods. *Statistics in Medicine* **17**(8): 873–890.

Pederson N, Jacoby GC, D'Arrigo RD, Cook ER, Buckley BM, Dugarjav C, Mijiddorj R. 2001. Hydrometeorological reconstructions for Northeastern Mongolia derived from tree rings: 1651–1995. *Journal of Climate* **14**(5): 872–881.

Peterson DW, Peterson DL. 1994. Effects of climate on radial growth of subalpine conifers in the North Cascade Mountains. *Canadian Journal of Forest Research* **24**(9): 1921–1932.

Peterson DW, Peterson DL. 2001. Mountain hemlock growth responds to climatic variability at annual and decadal time scales. *Ecology* **82**(12): 3330–3345.

Pike R, Bennett K, Redding T, Werner AT, Spittlehouse DL, Moore RD, Murdock TQ, Beckers J, Smerdon BD, Bladon KD, Foord VN, Campbell DA, Tschaplinski PJ. 2010. Climate change effects on watershed processes in British Columbia. In *Compendium of Forest Hydrology and Geomorphology in British Columbia*, Pike RG, Redding TE, Moore RD, Winkler RD, Bladon KD (eds). Ministry of Forests and Range Research Branch / FORREX Forest Research Extension Partnership: Victoria, BC; 699–747.

Puska L, Clements L, Chandler K. 2011. Climate change and food security on Vancouver Island: discussion paper. Report prepared by Vancouver Island Local Food Project, Victoria, BC. Retrieved from http://www.uvic.ca/research/centres/cue/assets/docs /Climate%20Change% 20and% 20Food%20Report.pdf

Rodenhuis DR, Bennett KE, Werner AT, Murdock TQ, Bronaugh, D. 2007. Climate overview 2007: Hydro-climatology and future climate impacts in British Columbia. Report prepared by the Pacific Climate Impacts Consortium, Victoria, BC. Retrieved from http://www.pacificclimate.org/sites/default/files/publications/Rodenhuis.ClimateOverview.Mar2009.pdf.

Sauchyn DJ, Vanstone J, St. Jacques J-M, Sauchyn R. 2014. Dendrohydrology in Canada's western interior and applications to water resource management. *Journal of Hydrology*. DOI:10.1016/j.jhydrol.2014.11.049.

Silvestri S. 2004. Stock Assessment of winter steelhead trout in Goldstream, Sooke, Trent and Tsable Rivers, 2004. Report prepared by BC Conservation Foundation: Greater Georgia Basin Steelhead Recovery Plan, Nanaimo, BC. Retrieved from http://a100.gov.bc.ca/apps data/ acat/documents/r5850/StockAssessmentReportFinal-NonPrintingCopy_1143403749 784_bb98440f95634e108ba9ff1269fd7f72.pdf

Smith DJ, Laroque CP. 1998. High-elevation dendroclimatic records from Vancouver Island. In *Proceedings of the Workshop on Decoding Canada's Environmental Past: Climate Variations and Biodiversity Change during the Last Millennium*, MacIver D, Meyer RE (eds). Atmospheric Service, Environment Canada: Downsview, Ont; 33–44.

Snedecor GW, Cochran WG. 1989. *Statistical Methods*. IA. Iowa State University Press: Ames.

Stahl K, Moore RD, Mckendry IG. 2006. The role of synoptic-scale circulation in the linkage between large-scale ocean–atmosphere indices and winter surface climate in British Columbia, Canada. *International Journal of Climatology* **26**(4): 541–560.

Stahle DW, Cook ER, Cleaveland MK, Therrell MD, Meko DM, Grissino-Mayer HD, Watson E, Luckman BH. 2000. Tree-ring data document 16th century megadrought over North America. *Eos, Transactions American Geophysical Union* **81**(12): 121–125.

Starheim CCA, Smith DJ, Prowse TD. 2013. Dendrohydroclimate reconstructions of July–August runoff for two nival-regime rivers in west central British Columbia. *Hydrological Processes* **27**(3): 405–420.

Stephens K, Ven der Gulik T, Heath T. 1992. Water, water everywhere: does British Columbia really need a water conservation strategy? *The BC Professional Engineer* **43**(8): 3–7.

Torrence C, Compo G. 1998. A practical guide to wavelet analysis. *Bulletin of the American Meteorological Society* **79**(1): 61–78.

Van Loon and Laaha AF, Laaha G. 2015. Hydrological drought severity explained by climate and catchment characteristics. *Journal of Hydrology* **256**(1): 3–14.

Wang T, Hamann A, Spittlehouse D, Aitken SN. 2006. Development of scale-free climate data for western Canada for use in resource management. *International Journal of Climatology* **26**(3): 383–397.

Wang T, Hamann A, Spittlehouse D, Murdock TN. 2012. ClimateWNA—high-resolution spatial climate data for western North America. *Journal of Applied Meteorology and Climatology* **51**(1): 16–29.

Watson E, Luckman BH. 2005. Spatial patterns of preinstrumental moisture variability. *Journal of Climate* **18**(15): 2847–2863.

Wigley TML, Briffa KR, Jones PD. 1984. On the average value of correlated time series, with applications in dendroclimatology and hydrometeorology. *Journal of Applied Meteorology* **23**(2): 201–213.

Wiles GC, D'Arrigo R, Barclay D, Wilson RS, Jarvis SK, Vargo L, Frank D. 2014. Surface air temperature variability reconstructed with tree rings for the Gulf of Alaska over the past 1200 years. *The Holocene* **24**(2): 198–208.

WinDENDRO. 1996. *WinDENDRO reference manual V. 6.1b, February 1996*. Re´gent Instruments, Que´bec.

Woodhouse CA, Gray ST, Meko DM. 2006. Updated streamflow reconstructions for the Upper Colorado River basin. *Water Resources Research* DOI:10.1029/2005WR004455.

Worrall J. 1983. Temperature–bud-burst relationships in amabilis and subalpine fir provenance tests replicated at different elevations. *Silvae Genetica* **32**(5/6): 203–209.

Yang YK, Huang Q, Liu Y, Wang WK, Wang YM. 2010. Advances in streamflow reconstruction using tree-ring data. *Advances in Water Science* **21**(3): 430–434.

Zhang Q, Hebda R. 2004. Variation in radial growth patterns of *Pseudotsuga menziesii* on the central coast of British Columbia, Canada. *Canadian Journal of Forest Research* **34**(9): 1946–1954.

